ELSEVIER

Sensors and Actuators A 49 (1995) 51–55

SENSORS AND ACTUATORS A PHYSICAL

A fiber-optic reflective displacement micrometer

Wen H. Ko *, Kow-Ming Chang, Gwo-Jen Hwang

National Chiao Tung University, Hsinchu, Taiwan

Received 14 March 1995; accepted 17 April 1995

Abstract

A simple fiber-optic reflection displacement micrometer with a sensitivity of 200 mV μm^{-1} and a resolution as low as 0.01 μm is reported with a theoretical explanation of the experimental results. The sensor consists of a pulsed LED light source and a pair (A and B) of identical receiving fibers and photodetectors that detects the light reflected from the surface being measured. The differential signal ($A-B$) of the detectors is proportional to the displacement of the surface relative to a null position. The light intensity variation of the source and the reflectance change of the surface are compensated when the ($A-B$) signal is divided by the sum ($A+B$). The resolution is limited by noise and interference (vibration of the base). A resolution of 0.01 μm can be achieved at narrow signal bands (d.c. to 3 Hz) excluding the low-frequency noise and vibration. The range, sensitivity and non-linearity can be adjusted according to the theory. The micrometer offers the advantages of non-contact, no electrical interference, simplicity, low cost and portability. It can be used in medical experiments and laboratory instruments.

Keywords: Displacement micrometers; Fiber optics

1. Introduction

Reflective fiber-optic sensors for displacement and pressure measurements exist in the literature for millimeter ranges [1–3]. Compensation methods using the ratio of the light in two fibers to reduce the effects of light-intensity variation have also been reported [4–7], where the fibers are arranged in a special pattern and are perpendicular to the reflecting surface. This article reports a simple arrangement of the fibers to achieve sub-micrometer resolution and different compensation methods. Low-cost fibers and optical components are used with common electronic circuits. A pulsed LED is used as the light source to reduce the power requirement and heat dissipation for portable applications.

This micrometer design offers the advantages of being non-contact, electrically safe, and immune from electromagnetic interferences, as well as having simplicity, low cost and portability with battery power. It can be used in medical experiments where electrical safety and portability are important, and in laboratory instruments to measure displacements and vibrations such as a step profile, deformation of a diaphragm or minute vibrations. It can also be used in industrial automation to measure displacement or vibration with a resolution down to 0.01 μm when the mounting of the sensor and the measured surface are rigidly connected to be free from relative motion interferences and the signal is either in a narrow band or outside the $1/f$ noise and vibration interference region [8,9].

2. Theory

Fig. 1 shows the fiber arrangement. Both receiving fibers are flat and perpendicular to the light path without recess from the shield. If the reflecting surface is a perfect mirror, the reflected light is equivalent to the transmitted light with the source, L, at the mirrored position L′ a distance z away. According to Yuan et al. [7], the intensity distribution function of the source at a position $Q(r, z)$ on a plane z away from the source and r away from the center of the light beam is

$$I(r, z) = I_0\{K_0/R^2(z)\}\ \exp[-r^2/R^2(z)] \quad (1)$$

where I_0 is the intensity of the light source, K_0 the loss in the input fiber, and $R(z)$ the effective radius of the output optical field. $R(z)$ is defined as

$$R(z) = [a_0 + kz^{3/2}\mathrm{tg}\theta_c] \quad (2)$$

where a_0 is the radius of the fiber core, θ_c the maximum incident angle for the fiber. and k a constant of the light source. The value of k was found experimentally to be 0.204

* Visiting professor from Case Western Reserve University, Cleveland, OH, USA.

SSDI 0924-4247(95)01018-V

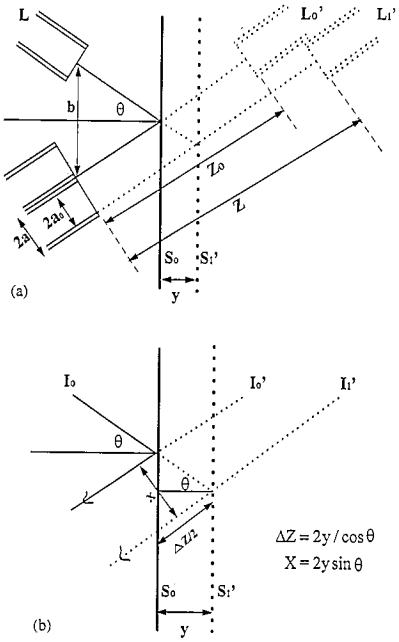

Fig. 1. (a) Arrangement of fibers of the micrometer. (b) Detailed positions of fibers and reflective surface.

for white light and 0.159 for He–Ne laser light [7]. If the reflecting surface is not perfect but with a reflection coefficient K_r, then the reflected light will be reduced by the factor K_r.

The transmitted light intensity at the end of the receiving fiber is [7]

$$I(r, z) = \iint_S \{[K_0 K I_0 \exp\left(-\sum n_i r_i\right) \times \exp(-r^2/R(z)^2]/(\pi R(z)^2)\, dS \quad (3)$$

where K is the loss in the receiving fiber, $\exp(-\Sigma n_i r_i)$ the loss in the medium [5,6], and S the receiving fiber core area. If the intensity at the receiving fiber center is used to represent the average intensity received and the reflectance coefficient is included, then the intensity received by the A and B fibers can be simplified to be [5,7]

$$A = I_1 = S_1 K_r K_0 K_1 I_0 \exp_1(n_i r_i) \times \exp[-(x+a)^2/R^2(z)]/R^2(z) \quad (4a)$$

$$B = I_2 = S_2 K_r K_0 K_2 I_0 \exp_2(-n_i r_i) \times \exp[-(x-a)^2/R^2(z)]/R^2(z) \quad (4b)$$

If the two receiving fibers are identical, then $K_1 = K_2$, $S_1 = S_2$, and $\exp_1(-n_i r_i) = \exp_2(-n_i r_i)$. The output $V = C(z)\cdot(A-B)/(A+B)$ is reduced to

$$V = C(z)\{\exp[-(x+a)^2/R^2] - \exp[-(x-a)^2/R^2]\}/\{\exp[-(x+a)^2/R^2] + \exp[-(x-a)^2/R^2]\} \quad (5)$$

where $C(z)$ is a constant and a function of z and R.

Referring to Fig. 1(b) the displacement of the reflecting surface y is related to x and z by

$$x = 2y \sin\theta \quad \text{and} \quad z = z_0 + 2y/\cos\theta \quad (6)$$

where z_0 is the initial reference value of z or the z value that gives equal I_1 and I_2. $z_0 = b/\sin\theta$, and it is determined by the spacing of the transmitting and receiving fibers, b, and the angle, 2θ, between them.

For very small y/z, a/z, and θ less than 45°, $(x+a) \ll R$ and the exponential function can be approximated by the first term in the series expression. Then

$$V = C(z)[2ax/R^2]/[1+(x/R)^2+(a/R)^2]$$

$$= C(z)[2ay\tan\theta/R^2]/[1+(2y\tan\theta/R)^2+(a/R)^2]$$

$$= [C(z)2a\tan\theta/(a_0+\text{tg}\,\theta_c z^{3/2})^2]y \quad (7)$$

Therefore, the output V is proportional to the displacement y. Furthermore, the output V is not a function of I_0, K_r, K_0, K_1, K_2 and S. This means that the effects of variations in light-source intensity and reflectivity are compensated. However, as y changes, not only the light received by the detector changes due to changes of x, but because the distance z also changes, which changes $R(z)$ according to Eq. (2). As z increases (even $y/z \ll R$), the scattering in the air path increases. Because R also increases with $z^{3/2}$, the light field of the LED fiber will spread over a wider area, thus the intensity is reduced. Therefore, dV/dy would decrease as y increases. This predicts that the output V varies nearly linearly with displacement y, but when the surface is moved toward the light source, the sensitivity (dV/dy) is larger, and when the surface is moved away from the source the sensitivity is smaller. This z-effect introduces non-linearity in the V–y characteristics of the device, if the range of y is large and both positive and negative displacements are to be measured. The non-linearity, defined as the maximum deviation from the linear line of V divided by the range of V, is larger for larger y-displacement and can be estimated from Eqs. (6) and (7).

3. Experimental setup

The experimental setup is shown schematically in Fig. 2. The LED is pulsed-on for 10–20 μs every millisecond to conserve power and reduce heat dissipation. the light is coupled to a fiber directed toward the reflecting surface. The reflected light is received by two identical fibers and photodetectors (A and B). The photocurrent is amplified and converted into a voltage, then it is fed to a sample-and-hold circuit

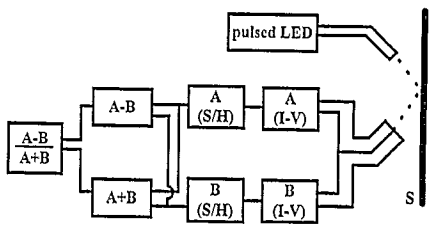

Fig. 2. Block diagram of the experimental setup.

in synchronation with the LED pulses. The signals A and B are processed to be $(A-B)$ and $(A+B)$; they are then fed to a divider circuit to give a V output proportional to the y displacement.

The probe of the micrometer contains all three fibers threaded through metal capillary tubes bent to the desired angle θ. θ values from 20 to 45° were tested with different separation b between the LED fibers and the receiving fibers as shown in Fig. 1. Results are similar except that the sensitivity changes. The fibers used are 0.5 mm and 1 mm plastic multimode fibers with a light shield but no special cladding. Their position relationship is fixed by molding compounds to determine a, b, and z_0. The surfaces of the fibers are flat to the surfaces of the metal tubes and are polished with fine emery papers. In the experiments, TEYT5500 phototransistors and Motorola MRD500 photodiodes were tested.

The position and the relative angle of the reflecting mirror are adjusted to give the desired z_0 and sensitivity. The probe and the reflecting mirror are mounted on a heavy substrate placed on a base, with a layer of foam rubber between the base and the laboratory table. A mechanical micrometer is used to control the displacement y.

4. Experimental results

4.1. Light-field distributions

Using the experimental setup as shown in Fig. 1, the values of a, b, z_0, and θ are 0.5, 4, 8 mm, and 20° respectively. Fig. 3(a) shows the LED light-intensity distribution (I_0 versus x) seen by a receiving fiber at $z=8$ mm. There is no change in z and the curve is symmetric on both sides of the reference position x_0. This curve has the shape of Eq. (4). The intensity of reflected light picked up by fibers A and B when y is changed is shown in Fig. 3(b); the intensity is normalized to the maximum value. Because z changes with y, the curve is not symmetrical with respect to the x_0 ($y=0$) point anymore. On the side where z is smaller than z_0 the curve is steeper (dI/dy larger), while on the other side where z is larger the curve is broader. This is the effect of z and R described in Section 2 and Eq. (7). Both Fig. 3(a) and (b) were recorded with 1 mm fibers. The relative shape would be the same for 0.5 mm fibers.

4.2. Linearity and sensitivity

In Fig. 3(b), the light intensity versus y curve of fiber B is also shown. Fiber B is displaced a distance $2a$ from the position of fiber A along the x direction. The crossover point, P, of the A and B curves corresponds to the reference point $y=0$ ($x=x_0$ and $z=z_0$), and the $(A-B)$ output is represented by the vertical lines at each y position. It is seen that because of the non-symmetric shape of curves A and B, the lengths of these lines are not exactly proportional to the y value. This is the cause of the non-linearity in the V–y characteristics shown

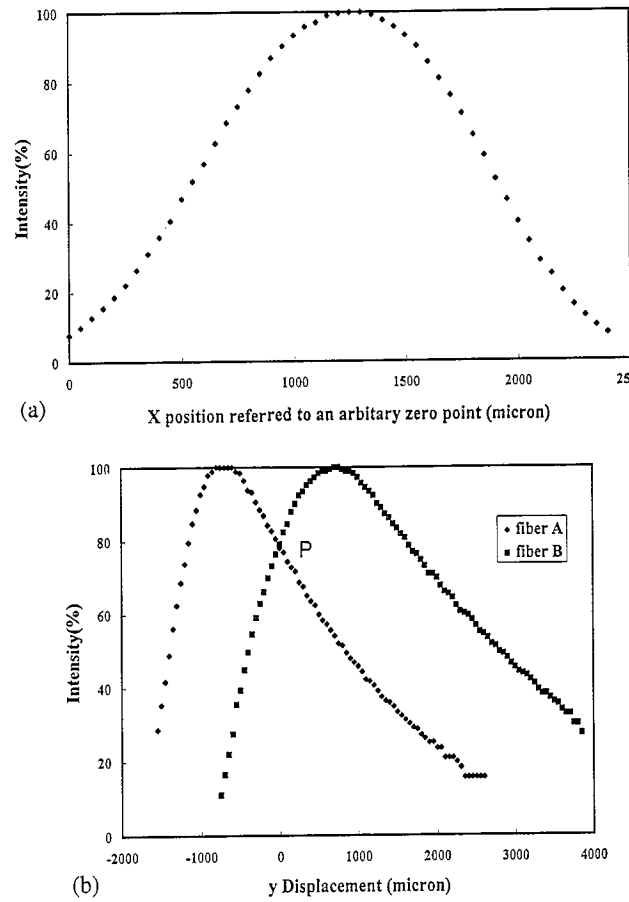

Fig. 3. (a) LED light intensity distribution curves. (b) Receiving fibers' intensity distribution curves.

in Fig. 4. Two typical V versus y characteristics are shown. These curves are obtained with different z_0, θ, and fiber diameters. Curve I is for 0.5 mm fibers with $z_0=4$ mm, $\theta=15°$, and MR-500 photodiodes. Curve II is for 1 mm fibers with $z_0=8$ mm, $\theta=25°$, and TEYT-5500 phototransistors. It is seen that the non-linearity, defined in Section 2, is less than 1% for $y_{max}=40$ μm with a sensitivity of 192 mV μm^{-1}. The non-linearity becomes 5% as y_{max} reaches 170 μm at a sensitivity of 53 mV μm^{-1}. Furthermore, most of the non-linearity occurs when $(-y)$ is greater than 100 μm.

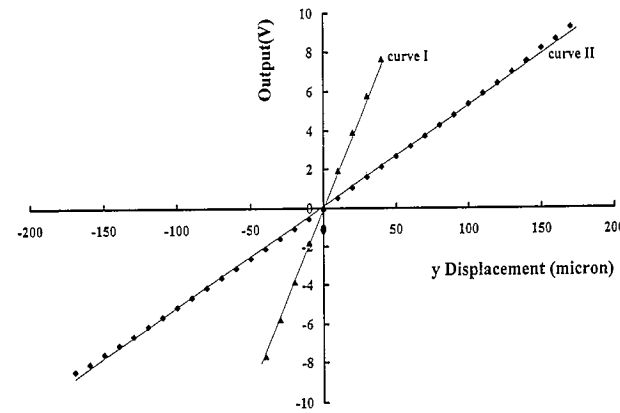

Fig. 4. Sensitivity and linearity of the micrometer: curve I for 0.5 mm fibers; curve II for 1 mm fibers.

4.3. Compensation effect

In order to evaluate the effectiveness of the compensation scheme using $(A+B)$ as the normalization factor for the output V, a fixed voltage of 3.0 V is used to replace the $(A+B)$ circuit output as the LED current is varied. The reflecting surface was kept at a constant position near the null point. The output of one I/V amplifier of a detector (A) is used as an indication of the light intensity from the LED. The results with and without the $(A+B)$ compensation are plotted in Fig. 5. When the LED light is decreased to 50%, the uncompensated sensitivity dropped to 60%, and the compensated sensitivity maintained above 92% of the original reference value.

4.4. Noise and resolution

The total gain of $(A-B)$ and the $(A-B)/(A+B)$ blocks is 100. The noise at the output across a 500 Ω resistor load with a 100 Hz low-pass filter is observed to have about a 20 mV peak on the laboratory table when the sensitivity is 50 mV μm^{-1}. A low-noise amplifier with variable low-pass filter is used to estimate the noise and the source. The result is shown in Table 1. On the laboratory table, the noise voltage from d.c. to 3 Hz is about 2.4 mV peak, therefore the resolution is about 0.1 μm when the signal voltage is twice the peak noise voltage. When the system is mounted on the optical bench with no room light, the sensitivity is about 200 mV μm^{-1} and the total noise voltage below 3 Hz is 1.0 mV. Then the resolution should be 0.01 μm for the signal voltage equal to twice the noise voltage or for 6 db S/N power ratio. However, the experiment to verify the estimation would require delicate operation and special equipment and has not been carried out at this time. Besides the low-frequency applications, if the signal is narrow banded and the frequency is higher than the $1/f$ noise range (say 100 Hz), then the noise again would be small and a resolution of 0.01 μm or better can be realized [8].

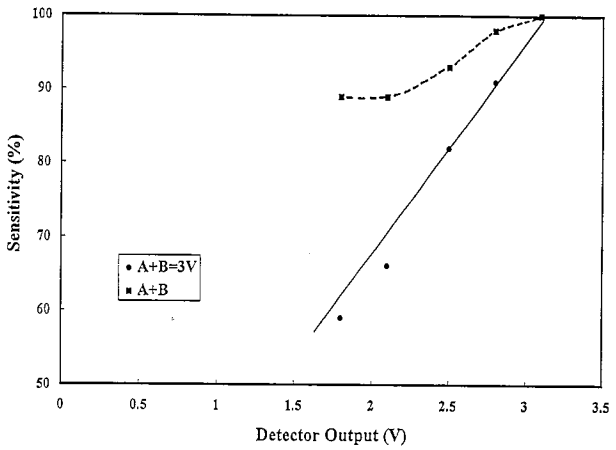

Fig. 5. Effects of compensation scheme. ●, $A+B=3$ V; ■, $A+B=$ actual values. Solid curve is uncompensated. Dashed curve is compensated.

Table 1
The noise of the device under different test conditions

Low-pass filter cut-off frequencies (Hz)	Total noise voltage (mV peak)	
	Laboratory table	Optical bench
0.03	0.05	0.01
0.10	0.12	0.05
0.30	0.40	0.10
1.0	1.0	0.40
3.0	2.4	1.0
10	8.0	2.4
30	12	5
100	20	10

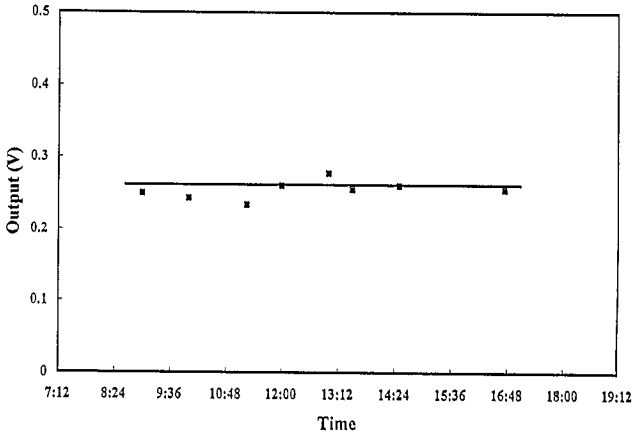

Fig. 6. Stability of the micrometer.

4.5. Time stability

The time stability over eight hours from 9:00 am to 5:00 pm on the laboratory table with room light on and one person assuming regular activities in the room was recorded as an indication of the time stability in the field. The data are shown in Fig. 6; the maximum variation of the baseline is ±25 mV or equivalent to 0.5 μm over 8 h.

5. Discussion and conclusions

A prototype optical micrometer has been designed and tested. The device has the advantages of being non-contact, electrically safe, and immune from electromagnetic interferences, as well as having simplicity, low cost and portability with battery power. The operating range can be adjusted from 50 to 500 μm full scale; however, the larger range would give larger non-linearity. The resolution depends on the signal frequency and its bandwidth. For the d.c. to 3 Hz band or a.c. signals above 100 Hz, a resolution of 0.01 μm is estimated. For fine resolution the vibration interferences have to be eliminated either by a special optical bench or by mounting the probe and the surface under test on the same rigid base so that any vibration from outside will affect the surface and the probe in exactly the same way. With proper mounting and

low-noise circuit elements, the device potentially can have a displacement resolution down to the 0.001 μm range.

The principle of operation and a theoretical explanation of the V–y characteristics are provided. The design considerations and trade-off are outlined for more refined sensors. The device is intended to be a portable probe for measuring deformations or vibrations of small amplitude. Possible applications may include: diaphragm deformation measurements for pressure and other sensors; minute vibration of instruments or machines; step height and surface roughness measurements; and medical measurements of sub-micrometer displacements and vibrations such as that of the human ossicular chain for hearing [8]. The device with a proper package may be used as a tool for dimensional control of manufactured parts with dimension accuracy down to the nanometer range.

A closed-loop light-intensity control scheme is being evaluated to eliminate the need for the divider block, which is the most expensive component in the system.

References

[1] R.O. Cook and C.W. Hamm, Fiber-optic displacement transducer, *Appl. Opt., 18* (1979) 3230–3241.

[2] T.E. Hansen, A fiber-optic microtip pressure transducer for medical applications, *Sensors and Actuators, 4* (1983) 545–554.

[3] W.H. Ko, Solid state transducers for biomedical research, *IEEE Trans. Biomed. Eng., BME-33* (1986) 153–162.

[4] G. Hull-Allen, Reflectivity compensation and linearization of fiber-optic proximity probe response, *SPIE Proc.*, Vol. 518, 1984, pp. 81–90.

[5] C.P. Cockshott and S.J. Pacaud, Compensation of optical fiber reflective sensor, *Sensors and Actuators, 17* (1989) 167–171.

[6] Yuan Libo and Qiu Anping, Fiber-optic diagram pressure sensor with automatic intensity compensation, *Sensors and Actuators A, 28* (1991) 29–33.

[7] Yuan Libo, Pan Jian, Yang Tao and Han Guochen, Analysis of the compensation mechanism of fiber-optic displacement sensor, *Sensor and Actuators A, 36* (1993) 177–182.

[8] W.H. Ko, A.J. Maniglia and R.X. Zhang, A preliminary study on the implantable middle ear hearing aid, *Proc. IEEE–EMBS 9th Ann. Conf., Boston, MA, USA, 1987,* Section 404.

[9] K.M. Chang, G.J. Hwang, W.H. Ko, T.H. Yeh and Y.N. Den, A fiber optic non-contact displacement micrometer, *1994 Int. Conf. Elect. Mat., Hsinchu, Taiwan, Dec. 1994,* Abstract C-5.5,95.

Biographies

Wen H. Ko is a visiting professor at the National Chiao Tung University, Taiwan, for the year 1994–95, and a professor emeritus of Case Western Reserve University, Cleveland, OH, USA, where he retired from regular teaching in July, 1993. Dr Ko is a member of the editorial board of *Sensors and Actuators*, *Sensors and Materials*, and *Microsystems Technologies*. He is a fellow of the IEEE BME society and AIMBE. His research interests are in solid-state devices, microsensors and microelectromechanical systems.

Kow-Ming Chang received the B.S. (with Great Distinction) degree in chemical engineering from National Central University, Chung-Li, Taiwan, in 1977 and the M.S. and Ph.D. degrees in chemical engineering from the University of Florida, Gainesville, in 1981 and 1985, respectively. His doctoral thesis concerned the processing technologies of compound semiconductors. In 1985, he joined the Department of Electronics Engineering and Semiconductor Research Center at the National Chiao Tung University, Hsin Chu, Taiwan, where he is presently a professor. From 1989 to 1990, he was a visiting professor in the Electrical Engineering Department, University of California, Los Angeles, where he was engaged in research on the system design of electron cyclotron resonance chemical vapor deposition (ECR–CVD) for developing low-temperature processing technology. He is now in charge of a 500 keV ion implanter and two UHV–ECR–CVD systems installed in the National Nano Device Laboratory (NDL) at the National Chiao Tung University. His research interests are in the physics, technologies, and modeling of heterojunction devices and optoelectronic devices, ULSI, CMOS, and MEMS technologies.

Dr Chang is a member of Phi Tau Phi, IEEE, AIChE and the Electrochemical Society.

Gwo-Jen Hwang received the B.S. degree in physics from the National Tsing-Hua University, Taiwan, in 1981 and the M.S. degree in physics from the State University of New-York at Buffalo, USA, in 1986. She has been with the Center for Measurement Standards in Taiwan since 1986. Her research is focused on the precision measurement of d.c. voltage and current. She is a part-time Ph.D. student at National Chiao Tung University and has been pursuing her research on MEMS since 1993.